Vol.26 No.4 **JOURNAL OF TROPICAL METEOROLOGY** Dec 2020

Article ID: 1006-8775(2020) 04-0428-13

Application of a Typhoon Initialization Scheme Based on the Incremental Analysis Updates Technique in a Rapid Update Cycle System

CHEN Feng (陈 锋), DONG Mei-ying (董美莹), JI Chun-xiao (冀春晓), QIU Jin-jing (邱金晶)
(Zhejiang Institute of Meteorological Sciences, Hangzhou 310008 China)

Abstract: Initialization of tropical cyclones plays an important role in typhoon numerical prediction. This study applied a typhoon initialization scheme based on the incremental analysis updates (IAU) technique in a rapid refresh system to improve the prediction of Typhoon Lekima (2019). Two numerical sensitivity experiments with or without application of the IAU technique after performing vortex relocation and wind adjustment procedures were conducted for comparison with the control experiment, which did not involve a typhoon initialization scheme. Analysis of the initial fields indicated that the relocation procedure shifted the typhoon circulation to the observed typhoon region, and the wind speeds became closer to the observations following the wind adjustment procedure. Comparison of the results of the sensitivity and control experiments revealed that the vortex relocation and wind adjustment procedures could improve the prediction of typhoon track and intensity in the first 6-h period, and that these improvements were extended throughout the first 12-h period of the prediction by the IAU technique. The new typhoon initialization scheme also improved the simulated typhoon structure in terms of not only the wind speed and warm core prediction but also the organization of the eye of Typhoon Lekima. Diagnosis of the tendencies of variables showed that use of the IAU technique in a typhoon initialization scheme is efficacious in resolving the spurious high-frequency noise problem such that the model is able to reach equilibrium as soon as possible.

Key words: typhoon initialization; vortex relocation; incremental analysis updates; numerical simulation; Lekima
CLC number: P456.7 **Document code:** A
https://doi.org/10.46267/j.1006-8775.2020.037

1 INTRODUCTION

Lorenz proved the importance of initial conditions (ICs) in numerical prediction. Especially in numerical prediction of tropical cyclones (TCs), adoption of a proper TC initialization method plays an equally important role as the implementation of an advanced model[1-2]. Small differences in the ICs (e. g., the position of a TC center and the strength of the TC) usually result in relatively large errors (Yan and Majewski[3]; Huang et al.[4]; Wan et al.[5]). Therefore, correction of deviations in the location and strength of an initial TC vortex is very important in TC forecasting, especially in the period before the TC makes landfall (Hendricks et al.[6]).

The majority of the lifetime of a TC is spent over an ocean where there is a general lack of observational data. Therefore, proper ICs such as the position of the TC center, minimum sea level pressure (MSLP) of the TC center, maximum wind speed (MWS) near the TC center, and radial distance of the maximum wind speed ($r_{\max}$) of the TC can be obtained only through limited observational information. Typically, such information is used to construct an artificial TC vortex using statistical empirical formulas and a dynamic conceptual model (called the TC bogus method), which is directly integrated into the background field to initialize a TC prediction (Kurihara et al.[7]; Lord[8]; Thu and Krishnamurti[9]; Wen et al. [10]). However, the TC bogus method usually causes imbalance between the initialized TC vortex and the dynamics of the forecast model owing to the lack of consideration of differences in typhoon structure. To construct a more realistic TC structure, Kurihara et al. proposed an improved method by decomposing a large-scale analysis into three components: the environmental flow and the symmetric and asymmetric parts of the vortex circulation[11-12]. The symmetric part is generated by the TC bogus method, while the asymmetric part is taken from the previous 12-h forecast. Both symmetric and asymmetric parts are added to the environmental flow to construct the final ICs (Bender et al.[13]). Based on this technique, a vortex relocation technique is then commonly used in numerical predictions of TCs (Liu et al.[14]; Yuan et al.[15]), which partly solves erroneous

---

Received 2020-05-18 **Revised** 2020-08-15 **Accepted** 2020-11-15

Funding: Science and Technology Project of Zhejiang Province (LGF20D050001); East China Regional Meteorological Science and Technology Innovation Fund Cooperation Project (QYHZ201805); Meteorological Science and Technology Project of Zhejiang Meteorological Service (2018ZD01, 2019ZD11)

Biography: CHEN Feng, Ph. D., primarily undertaking research on numerical prediction and data assimilation.

Corresponding author: DONG Mei-ying, e-mail: dongmy_zj@163.com

spin-up problems caused by inconsistencies between ICs and model dynamics and physics.

The problem of imbalance between the initialized TC vortex and the dynamics of the forecast model is not totally resolved by the above approach because the symmetric part of the vortex circulation, which remains generated using empirical formulas and a dynamic conceptual model, still has differences to the actual typhoon structure. Several attempts have been made to reduce these differences. For example, Xiao et al., Pu and Braun, Huang et al. and Yuan et al. did not use the bogus data directly; instead, they incorporated the data through a bogus data assimilation (BDA) system to generate all the other variables by integrating the forecast model[16-19]. Qu et al., Yuan et al., and Hsiao et al. performed vortex relocation and intensity adjustment based on the background field from a weak TC vortex predicted by the model, which considerably improved the typhoon track prediction[15; 20-22]. Liang and Wang proposed a model constrained 3DVAR technique to construct a more coordinated vortex structure[23], which was then applied in the GRAPES-TCM by Huang and Liang[24]. Although the BDA method uses the equilibrium constraints of the variational system, remaining inconsistencies between the ICs and model dynamics can cause spurious high-frequency noise and therefore further work is required on this topic.

The incremental analysis updates (IAU) technique is an effective method with which to resolve the spurious high-frequency noise problem such that a model can reach equilibrium as soon as possible with minimal demand on computing resources (Bloom et al.[25]; Polavarapu et al.[26]; Takacs et al.[27]). The IAU technique has been used widely in applications in the atmospheric and oceanic fields (Lee et al.[28]; Ourmières et al.[29]; Benkiran and Greiner[30]; Lei and Whitaker[31]; Xu et al.[32]). For example, Lee et al. added the analysis increment from the MM5-3DVAR system to a model integration using the IAU method, which resolved the spin-up problem associated with hydrometeors and significantly improved precipitation forecasting[28]. Lei and Whitaker proposed a four-dimensional IAU approach that used the ensemble Kalman filter (EnKF) to combat the imbalance caused by data assimilation[31]. In the work by Xu et al., the IAU technique was introduced successfully into a typhoon initialization scheme to resolve the inconsistencies in the ICs generated by a typhoon initialization scheme and model dynamics[32].

The Weather Research and Forecasting model (WRF, Skamarock et al.[33]; http://www2.mmm.ucar.edu/wrf/users) is currently running at the Zhejiang Institute of Meteorological Sciences as the operational mesoscale numerical weather prediction system (Chen et al.[34]) and rapid refresh system (Qiu et al.[35]). However, in both operational systems, especially the latter, TC prediction has obvious errors due to the lack of a typhoon initialization scheme. First, large errors in numerical prediction of TCs are found owing to inaccurate positioning of TC centers in the ICs. Although observations could be assimilated to improve the quality of ICs, which is the advantage of the rapid refresh system, the effect would only be small because of the limited availability of observational data over the oceans. Second, even if vortex relocation and intensity adjustment procedures were applied to the initial fields, the imbalances that include the dynamically inconsistent and spurious high-frequency noise problem would remain serious. Observational data is incorporated into the model via data assimilation or typhoon initialization schemes, which cause the imbalances and increase the model spin-up time. Therefore, it is necessary to establish the feasibility of using the IAU technique to overcome this problem.

In this study, a typhoon initialization scheme incorporating the IAU technique was applied to the operational rapid refresh system to both reduce the model spin-up time and combat the imbalance in the analysis following vortex relocation and intensity adjustment. The following sections of this paper are organized as follows. Section 2 describes the methodology of the proposed scheme. In section 3, the operational rapid refresh system and the numerical experiments are introduced. The impacts of the new scheme on the prediction of TC Lekima (2019) are discussed in section 4. In the final section, a discussion and the conclusions are presented.

2 METHODOLOGY

The proposed typhoon initialization scheme is based on the IAU technique. There are three steps to achieving typhoon initialization using this scheme. First, a commonly used vortex relocation method is chosen to separate the background field into the TC vortex and the environmental flow. Then, the TC vortex is relocated to its observed location. Subsequently, the wind speed of the TC vortex is adjusted according the observed MWS near the TC center, and then the adjusted TC vortex is added back into the environmental flow to obtain the updated ICs with the revised TC position and corrected TC intensity. Finally, the increments, obtained by comparing the new field and the background field before the implementation of the vortex relocation and wind adjustment procedures, are incorporated into the model's prognostic equations using the IAU method.

2.1 *Vortex relocation*

The vortex relocation method primarily follows Kurihara[12]. Schematically, the scheme used to construct a realistic initial field can be expressed as follows:

$$H' = H_E + H_V' = H - H_V + H_V', \qquad (1)$$

where H/H' is the background / analyzed field before /

after the vortex relocation process, H_E is the environmental field (or large-scale circulation field), H_V is the vortex component (or storm component) of the storm separated from the background field, and $H_V^{'}$ is the vortex component with the TC position adjusted.

The most important element of the procedure is the separation of the TC vortex against its environmental flow from the background fields, which can be divided into the following steps.

(i) Identify the initial TC position and covering radius of TC vortex in the background. The geopotential height field at 850 hPa is used to determine the location of TC center. Then, the angular mean wind (AMW) is calculated. As the radial distance increases, the AMW will increase monotonously to a maximum value (where the radial distance is called $r_{\max}$) and then decrease monotonously. The covering radius r_0 is defined as the radial distance at which the AMW is equal to a predetermined value (set at 3 m s^{-1} here) at the first time when the radial distance increases after $r_{\max}$.

(ii) Separate the perturbation field from the background field using a twice-smoothing filter technique. A three-point smoothing algorithm is performed first longitudinally and then zonally on the background field with the same smoothing coefficient as used by Yuan et al.[15] to obtain the perturbation field H_D.

(iii) Separate the TC vortex from the perturbation field by applying a column filter technique:

$$H_V(r,\theta)=\left[1-E(r)\right]\left[H_D(r,\theta)-\overline{H_D(r_0)}\right], \tag{2}$$

where r is the radial distance from the TC center, θ is the azimuth of the TC system, r_0 is the covering radius of the TC vortex, $\overline{H_D(r_0)}$ is the angular mean of H_D at the point of r_0, and $E(r)$ is the column filter function, which can be expressed as follows:

$$E(r)=\frac{exp\left[-\left(r_0-r\right)^2/l^2\right]-exp\left[-r_0^2/l^2\right]}{1-exp\left[-r_0^2/l^2\right]}, \tag{3}$$

where l is the shape parameter of $E(r)$ (here, $l=r_0/5$ in this work).

(iv) Obtain the large-scale environmental field:

$$H_E=H-H_V. \tag{4}$$

Finally, the obtained vortex component H_V is moved to the corrected position where its vortex center agrees with the observed TC center, which is called the vortex component with the TC position adjusted $H_V^{'}$.

2.2 *Wind speed adjustment*

The wind speed adjustment follows Xu et al.[32]. According to Equation (4), the wind field with the TC position adjusted can be expressed as follows:

$$\begin{cases} u^{'}=u_E+u_V^{'} \\ v^{'}=v_E+v_V^{'} \end{cases}, \tag{5}$$

where $u^{'}$ and $v^{'}$ are the zonal and meridional wind components of $H^{'}$, u_E and v_E are the zonal and meridional wind components of the large-scale environmental field H_E, and $u_V^{'}$ and $v_V^{'}$ are the zonal and meridional wind components of the vortex component with the TC position adjusted $H_V^{'}$, respectively.

The wind speed adjustment is conducted by multiplying a coefficient:

$$\begin{cases} u_c^{'}=u_E+\beta\times u_V^{'} \\ v_c^{'}=v_E+\beta\times v_V^{'} \end{cases}, \tag{6}$$

where $u_c^{'}$ and $v_c^{'}$ are the zonal and meridional wind components after adjustment, respectively. Obviously, the surface MWS calculated from $u_c^{'}$ and $v_c^{'}$ should be equal to the observed one V_{obs}:

$$u_{c,r_0}^{'}{}^2+v_{c,r_0}^{'}{}^2=\left(u_E+\beta\times u_V^{'}\right)^2+\left(v_E+\beta\times v_V^{'}\right)^2=V_{\text{obs}}, \tag{7}$$

where $u_{c,r_0}^{'}$ and $v_{c,r_0}^{'}$ are the zonal and meridional wind components after adjustment at the point where the surface wind is maximum, respectively. Thus, coefficient β can be solved as follows:

$$\beta=\frac{-\left(u_Eu_V^{'}+v_Ev_V^{'}\right)+\sqrt{\left(u_Eu_V^{'}+v_Ev_V^{'}\right)^2-\left(u_V^{'}{}^2+v_V^{'}{}^2\right)\left(u_E{}^2+v_E{}^2-V_{\text{obs}}{}^2\right)}}{\left(u_V^{'}{}^2+v_V^{'}{}^2\right)}, \tag{8}$$

It should be noted that coefficient β is calculated at the surface. Based on practical experience, it is known that the wind speed error decreases gradually as the height increases. Therefore, coefficient β should change linearly to a value of 1 at 500 hPa, which means that the wind speed in the lower (higher) levels has undergone large (small) correction.

2.3 *Typhoon initialization scheme based on IAU*

technique

The IAU technique incorporates analysis increments into a model integration in a gradual manner. The analysis increments are treated as constant additional forcing terms in the model's prognostic equations over a certain time window:

$$\frac{\partial F}{\partial t} = \cdots + \frac{F_a - F_b}{\tau}, \tag{9}$$

where F is the prognostic variable, F_a is the analyzed field with the vortex relocated, F_b is the background field before the vortex is relocated, and τ is the relaxation time window. Bloom et al. proved that the IAU procedure has the attractive properties of a low-pass time filter that can affect the response of a model to the analysis increments[25]. By progressive incorporation of the analysis increments, the IAU method removes high-frequency noise (Lee et al.[26]).

3 MODEL AND NUMERICAL EXPERIMENTS

The prediction system used in this study was the Zhejiang WRF-ADAS Rapid Refresh System (ZJWARRS, Qiu et al.[35]). This system uses the WRF model version 4.0.2 as its prediction model, and takes the Advanced Regional Prediction System (Xue et al.[36] 2000; Xue et al.[37]) Data Assimilation System (ADAS) (Brewster[38]) as its system for data assimilation. The ZJWARRS was first established in 2013 with a 3-h assimilation cycle in which a new analysis was produced at 3-h intervals using the previous 3-h forecast as the background field. In this work, a cold-start was conducted once daily at 18:00 UTC using the ICs and boundary conditions from the forecast of the Integrated Forecasting System of the European Centre for Medium-Range Weather Forecasts starting at 12:00 UTC (https://www.ecmwf.int/en/forecasts/datasets/set-i). This system absorbs many different observations (e.g., SYNOP, METAR, SHIP, Rawinsonde, Wind profile, AMDAR, Doppler radar reflectivity, and radial velocity) and produces 24-h forecasts from the time of data assimilation (extended to 36 h in this work). A two-level nested grid was used in which the parent domain (9-km resolution) covered East China and the second domain (3-km resolution, 35 vertical levels) covered Zhejiang Province. Further detailed information can be found in Qiu et al.[35]. The ZJWARRS, which is now the operational mesoscale data assimilation and numerical prediction system run at the Zhejiang Meteorological Service, is designed to provide frequently updated numerical forecast guidance. Although observations can be assimilated to improve the quality of the ICs, which is one of the principal advantages of the rapid refresh system, the effect would be small because of the limited availability of observational data over the ocean. Therefore, a typhoon initialization scheme is necessary for typhoon prediction using the ZJWARRS.

Three experiments were designed to evaluate the effect of the typhoon initialization scheme on the simulation of TC Lekima (Fig. 1). The control experiment (Exp. CTL) without any typhoon initialization scheme took the 3-h forecast of the final cycle as its ICs and performed continuous 36-h integration. The vortex relocation experiment (Exp. VOR) performed the vortex relocation and wind speed adjustment processes based on the 3-h forecast of Exp. CTL and then performed 33-h integration. Observed TC information, including the longitude/latitude of TC center, minimum sea level pressure of the TC center, maximum wind speed near the TC center, and radial distance of the maximum wind speed of the TC, was combined into the background field in Exp. CTL. The experiment incorporating the new scheme (Exp. IAU) had the same configuration as that of Exp. CTL, except that it added increments based on the IAU technique during the first 3-h time window. The increments were calculated by comparison of the analysis field after the vortex relocation in Exp. VOR and the original field of the 3-h forecast of Exp. CTL. All three experiments were conducted at 3-h intervals using the rapid refresh technique, and the 36-h forecasts were integrated within each cycle. The differences between Exp. VOR and Exp. CTL determined whether it was necessary to adjust the typhoon vortex according to the actual observational information. Information was absorbed in Exp. VOR at one time, whereas Exp. IAU absorbed information gradually throughout the 3-h time window.

4 RESULTS

Typhoon Lekima (2019), the strongest typhoon to make landfall in China in 2019, was chosen to evaluate the new typhoon initialization scheme in this work. Lekima was detected as a tropical storm in the Northwest Pacific on August 4, 2019. It then strengthened to become a super typhoon by the evening of August 7, and eventually made landfall on the coast of Wenling County (Zhejiang Province) at approximately 17:45 UTC on August 10. Eight cycles were conducted using the ZJWARRS at 3-h intervals with start times from 18:00 UTC August 8 to 15:00 UTC August 9, 2019. Thus, the impact of the typhoon initialization scheme was investigated based on these simulations of the typhoon on the day before it made landfall.

4.1 *Illustrations of decomposition, wind speed adjustment, and vortex relocation*

Typhoon initialization begins with decomposition of the original background field. One of the cycles in Exp. VOR (i.e., 21:00 UTC August 8, 2019) is selected to illustrate the wind field decomposition and vortex relocation procedure, and their impact on the TC initial field. The original wind field at 850 hPa (Fig.2a) is separated into the large-scale environmental component (Fig. 2b) and the vortex component (Fig. 2c). It can be seen from Fig. 2b that the environmental

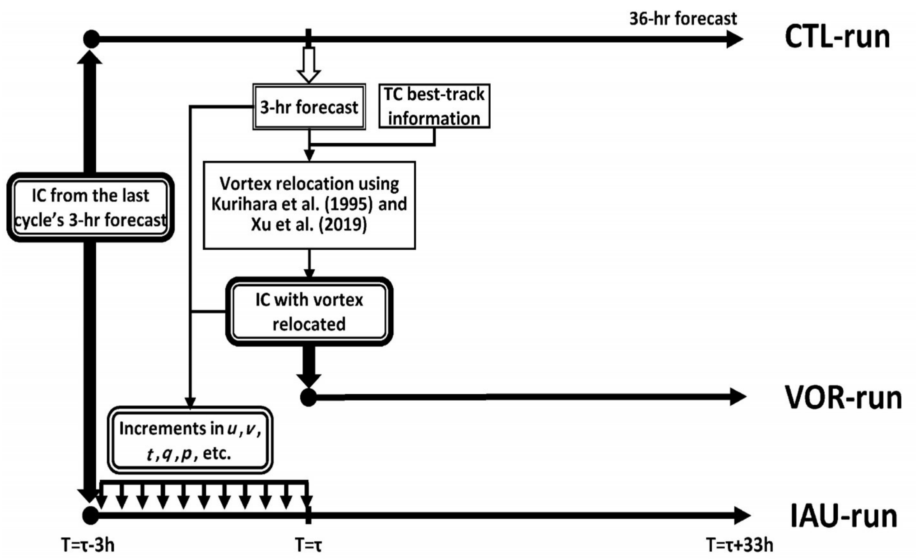

Figure 1. Schematic of the experimental design.

wind flow near the TC center is mainly southerly and southeasterly. Meanwhile, a complete independent cyclonic circulation is separated from the environmental flow in Fig. 2c. Other levels (e.g., 500 hPa) show similar results as those displayed here for the 850-hPa level, except that the southwestward steering flow is more evident. These results match the observations and indicate that the decomposition procedure is correct. The new vortex component is then obtained by relocation of the TC center to the observed position, and the maximum wind speed is adjusted to that observed. The new wind field is obtained by adding the new vortex component to the environmental component (Exp. VOR), which has marked differences to the original (Exp. CTL, Fig. 2d).

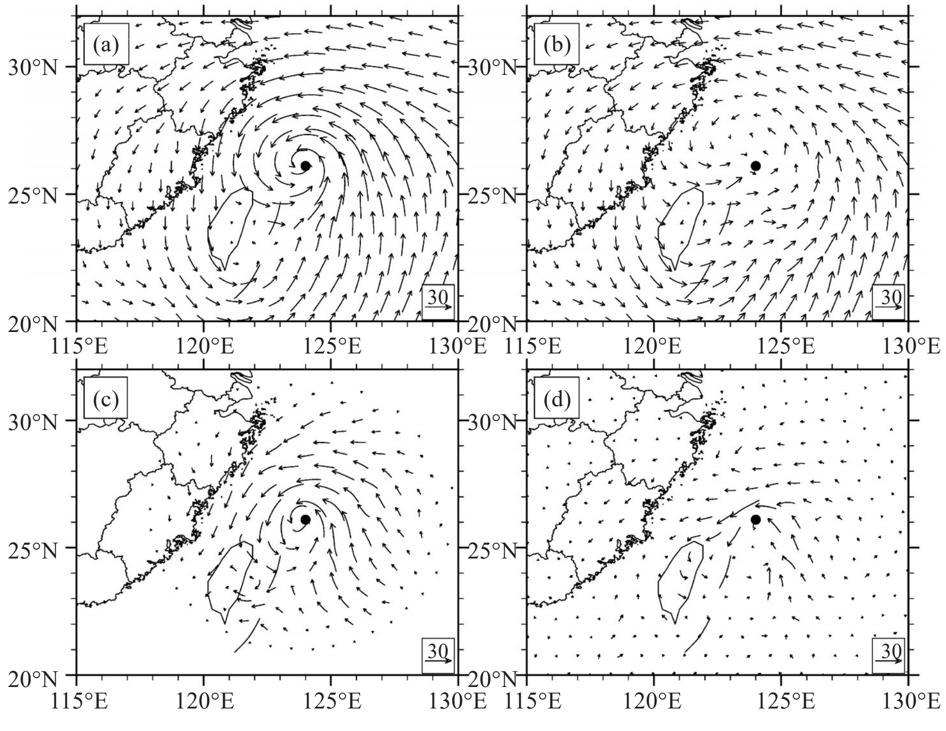

Figure 2. Decomposition of Typhoon Lekima at 850 hPa at 21:00 UTC on August 8, 2019 for the vortex relocation: (a) the original total background flow, (b) the large-scale environmental component, (c) the vortex component, and (d) the difference between the new total flow and the original one.

The simulated SLP and wind at 10 m height associated with Typhoon Lekima at 21: 00 UTC on August 8, 2019, obtained from the three experiments, are shown in Fig. 3. It is evident from comparison of Exp. VOR (Fig. 3b) and Exp. CTL (Fig. 3a) that the simulated typhoon position matches the observations much better following the vortex relocation procedure, and that the wind speed near the TC center is much greater following the wind adjustment procedure. In addition, the MSLP is evidently lower (950 .vs. 954 hPa) and the MWS higher (53.5 .vs. 33.7 m s^{-1}) when comparing the results of Exp. VOR with those of Exp. CTL, meaning that the typhoon intensity has become stronger and closer to that observed. The results of Exp. IAU are somewhere in between those of Exp. CTL and Exp. VOR. However, the variables are more balanced in Exp. IAU than in Exp. VOR (further analysis is presented in section 4.3). This reflects the impact of the one-time addition of the increments between Exp. VOR and Exp. CTL versus the gradual addition of the increments throughout the 3-h time window in the IAU technique.

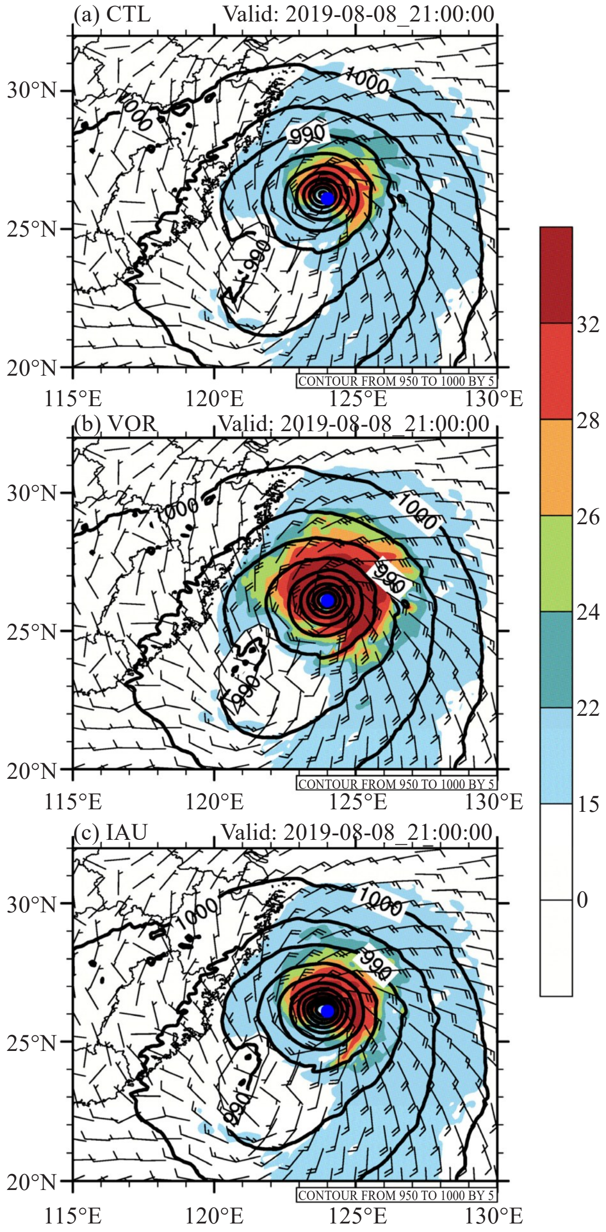

Figure 3. Simulated sea level pressure (thick solid contour, hPa), wind speed (shading, m s^{-1}), and wind barbs at z=10 m for Typhoon Lekima at 21:00 UTC August 8, 2019 from (a) Exp. CTL, (b) Exp. VOR, and (c) Exp. IAU. The approximate center of the observed typhoon (blue dot) is indicated near the domain center in each panel.

4.2 *Improvements on typhoon track and intensity*

The average errors in the typhoon track and intensity of all the cycles of the ZJWARRS are statistic for each forecast time extended to 36 h for Exp. CTL, Exp. VOR, and Exp. IAU (Fig. 4). Following vortex relocation and wind speed adjustment at the analysis time, the typhoon position is obviously moved to the correct position and the track error is decreased markedly in Exp. VOR when compared with Exp. CTL. In the IAU technique, the increments at the analysis time are added gradually during the previous 3-h time window at every model step, which leads to improvement in the typhoon track prediction by Exp. IAU when compared with that of Exp. CTL. It is worth noting that the track prediction is improved throughout most of the forecast period in Exp. IAU, whereas most of the improvement appears in the first 6-h period in Exp. VOR. This means that the vortex relocation procedure improves the track prediction mainly in the first 6-h period of the forecast, but the IAU technique can extend this improvement through reducing the imbalance between the ICs and model dynamics.

Results similar to those relating to the typhoon track were found to be related to the intensity prediction. The MSLP and MWS errors in Exp. VOR and Exp. IAU are smaller than those in Exp. CTL, and these improvements are obvious in the first 6–12 h. The intensity prediction in Exp. IAU seems to be slightly better than that in Exp. VOR, especially for the MSLP prediction (Fig. 4b). It should be noted that the MWS error shows a sharp decrease at the analysis time in Exp. VOR when the speed adjustment technique is applied; however, it recovers quickly owing to the imbalance between the wind field and other variables. This indicates that the big shock related to the one-time addition of the increments could be alleviated by using the IAU technique.

Improvement in typhoon intensity prediction can be found in all eight cycles of the ZJWARRS. Comparison of the MSLP error at the typhoon center simulated at the different cycles of the three experiments is shown in Fig. 5. The greatest improvement of approximately 4.8 hPa in Exp. VOR disappears after the first 12-h period, whereas the improvement in Exp. IAU (approximately 8.4 hPa) persists for a little longer. In general, the vortex relocation and wind speed adjustment procedures

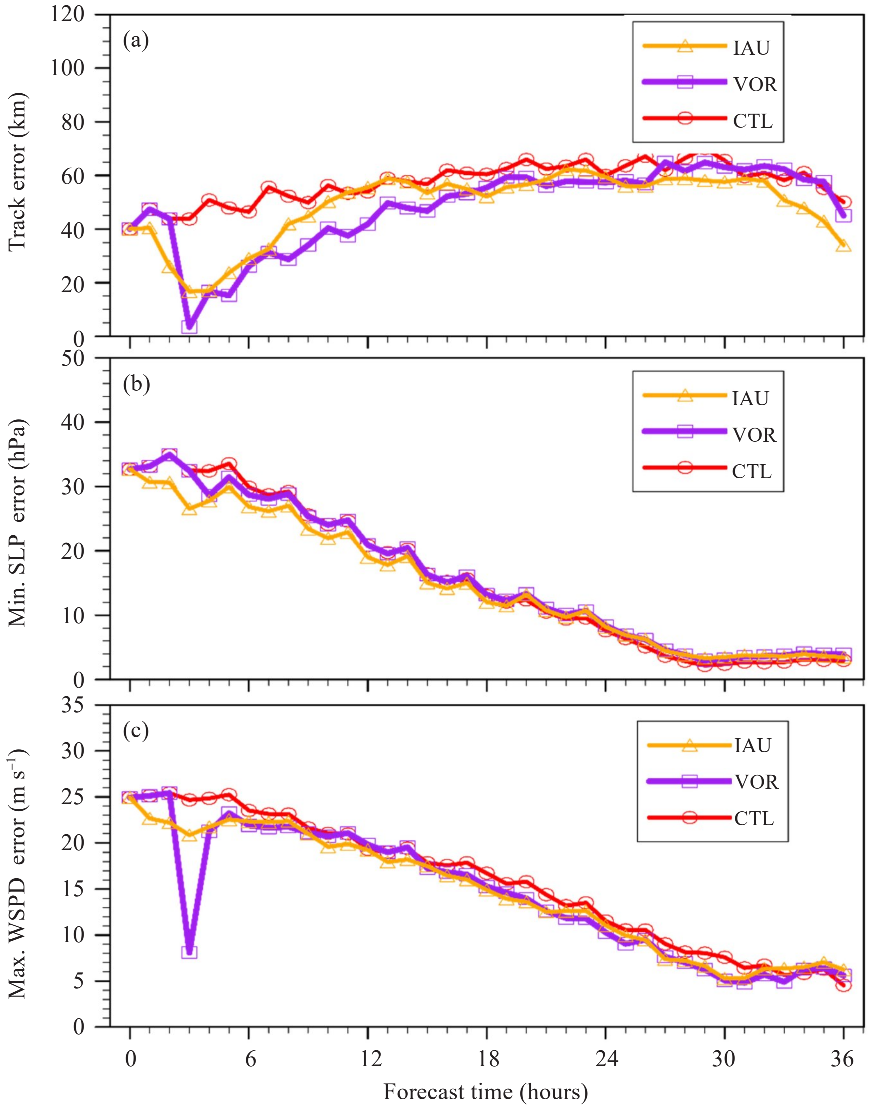

Figure 4. Influence of initialization on the forecast of Typhoon Lekima: (a) average track error (km), (b) average error of minimum sea level pressure at the typhoon center (hPa), and (c) average error of maximum wind speed near the typhoon center (m s^{-1}).

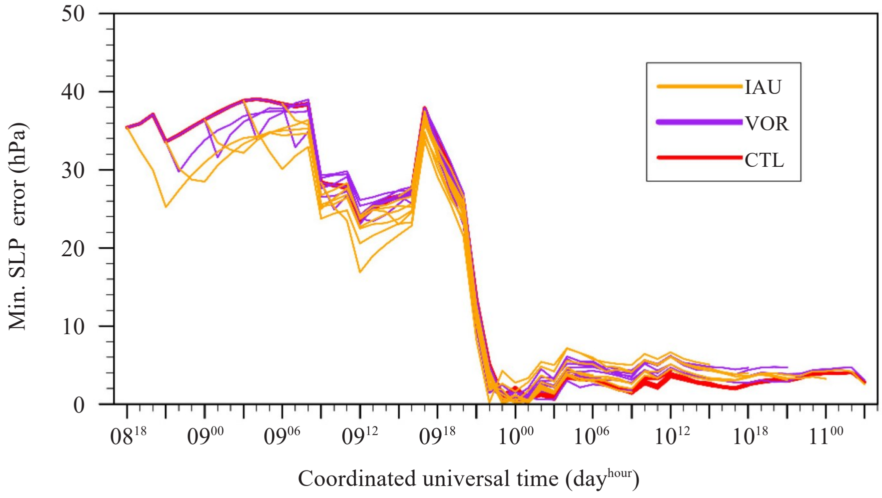

Figure 5. Comparison of minimum sea level pressure error (hPa) at the typhoon center simulated by the different cycles of the three experiments.

clearly improve the predictions of the track and intensity of Typhoon Lekima, and these improvements become larger and persist for longer when using the IAU technique.

4.3 *Typhoon structure comparison*

Typhoon structure is another important part of TC prediction. Again, one cycle that started at 18:00 UTC August 8, 2019, is selected to illustrate the comparison of the typhoon structure among the three experiments. Zonal vertical cross sections along the typhoon center showing wind speed and temperature deviations at 3, 6, and 12 h after the model started are illustrated in Fig. 6. At 21:00 UTC (3 h after the model started), larger wind speeds can be found in Exp. VOR and Exp. IAU than in Exp. CTL. Especially in Exp. VOR, the MWS is 53.6 m s^{-1}, which matches the observation (60.0 m s^{-1}) more closely than that in Exp. CTL (approximately 33.7 m s^{-1}). However, the warm core of the TC in Exp. VOR is similar (approximately 7.5 K) to that in Exp. CTL, which shows great inconsistency between wind speed and temperature after the implementation of the vortex relocation and wind adjustment procedures. In Exp. IAU, this inconsistency is much smaller, i. e., the MWS is increased (from 33.7 m s^{-1} in Exp. CTL to 37.9 m s^{-1} in Exp. IAU) and the warm core is stronger (from 7.5 K in Exp. CTL to 8.5 K in Exp. IAU). Owing to the inconsistency in the variables after implementation of the vortex relocation and wind speed adjustment procedures, the simulated MWS drops rapidly in Exp. VOR from 53.4 m s^{-1} at 21:00 UTC on August 8 to 34.1 m s^{-1} at 00:00 UTC on August 9, and then to 32.4 m s^{-1} at 06:00 UTC on August 9. The MWS in Exp. IAU is 37.9, 34.3, and 34.7 m s^{-1} at 21:00 UTC on August 8, 00:00 UTC on August 9, and 06:00 UTC on August 9, respectively, which is a more reasonable trend of change. Furthermore, the warm core in Exp. IAU is also more reasonable in comparison with that in Exp. CTL and VOR at 00:00 and 06:00 UTC August 9. These results show the advantages of using the IAU technique in typhoon structure prediction.

Comparison of the simulated radar composite reflectivity, 1-h accumulated precipitation, and vertical accumulated hydrometeors with the observed FY2G

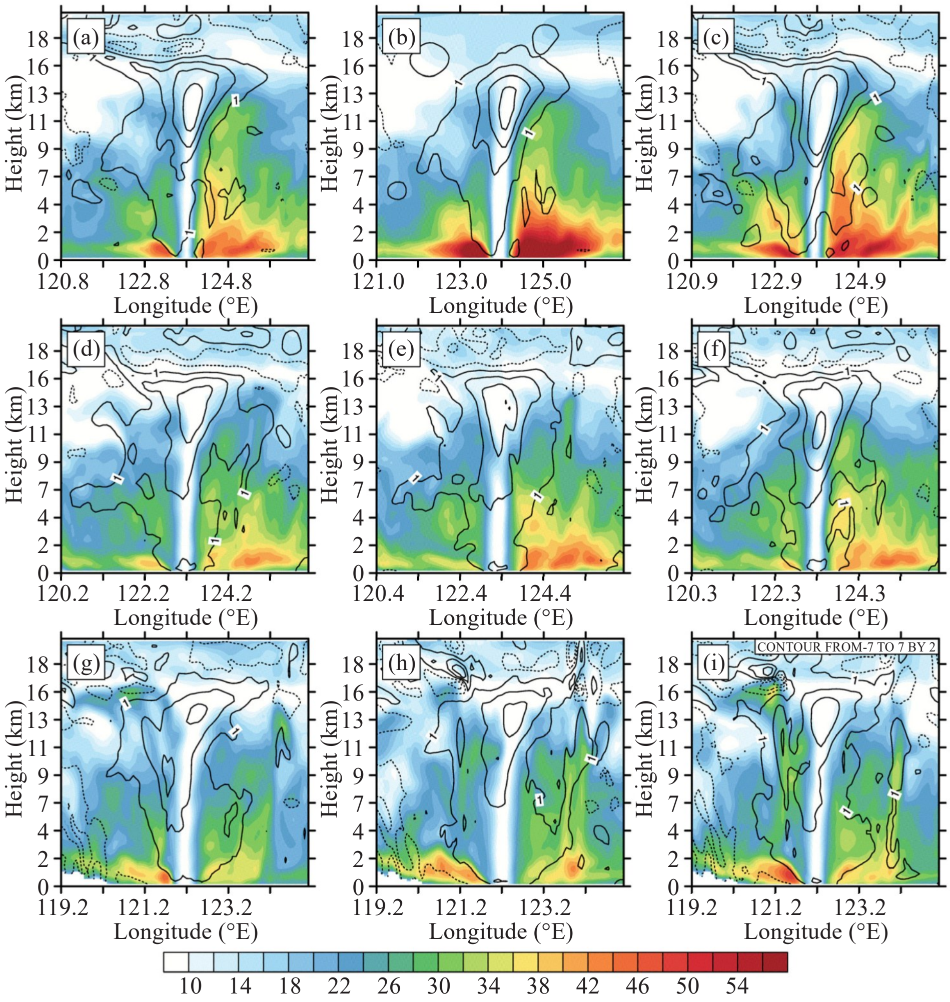

Figure 6. Zonal vertical cross sections along the typhoon center showing wind speed (shading, m s^{-1}) and temperature deviations (solid contour for positive, dash contour for negative, *K*). The model was initialized at 18:00 UTC on August 8, 2019: (a)-(c) are 3-h forecasts, (d)-(f) are 6-h forecasts, and (g)-(i) are 12-h forecasts. Results are from (a), (d), and (g) Exp. CTL; (b), (e), and (h) Exp. VOR; and (c), (f), and (i) Exp. IAU.

black body temperature (TBB) radar composite reflectivity, and China Meteorological Administration Land Data Assimilation System (CLDAS) - analyzed precipitation is shown in Fig. 7. All three experiments successfully reproduced the distribution of the spiral rain band; however, the organization of the eye of the typhoon was simulated better in Exp. IAU (Fig. 7f). A closer view of the eye of Typhoon Lekima is presented in Fig. 8. The observed radar reflectivity shows a double-eyewall structure (Fig. 8b), although the reflectivity on the southern and eastern sides is missing owing to radar range limitations. Similar clues can also be found in the TBB and accumulated precipitation shown in Fig. 8a and 8c, respectively. The spiral rain band on the northern side is more obvious in Exp. IAU (Fig. 8d-f), and a quasi-double-eyewall structure is reflected in the simulated 1-h accumulated precipitation (Fig. 8i) and vertical accumulated hydrometeors (Fig. 8l). This means that the reproduction of the vortex structure by Exp. IAU was better than those by Exp. CTL and Exp. VOR.

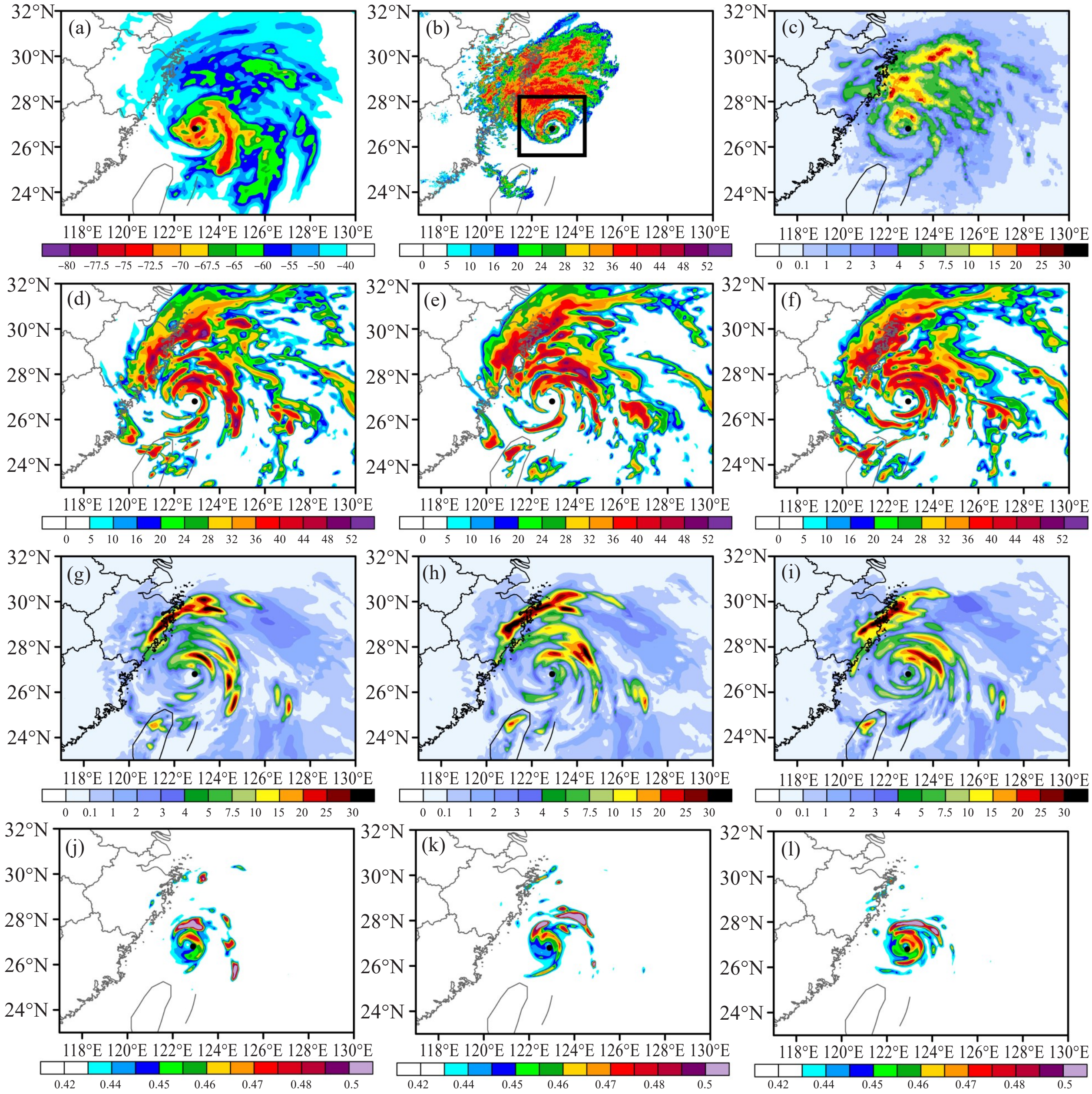

Figure 7. Comparison of (a) FY2G TBB (℃), (b) observed radar composite reflectivity (dBZ), and (c) CLDAS merged precipitation (mm) and simulated radar composite rreflectivity (dBZ) from (d) Exp. CTL, (e) Exp. VOR, and (f) Exp. IAU, simulated 1-h accumulated precipitation from (g) Exp. CTL, (h) Exp. VOR, and (i) Exp. IAU, and simulated vertical accumulated hydrometeors from (j) Exp. CTL, (k) Exp. VOR, and (l) Exp. IAU at 03:00 UTC on August 9, 2019. The black rectangular box in (b) refers to the core area of Typhoon Lekima.

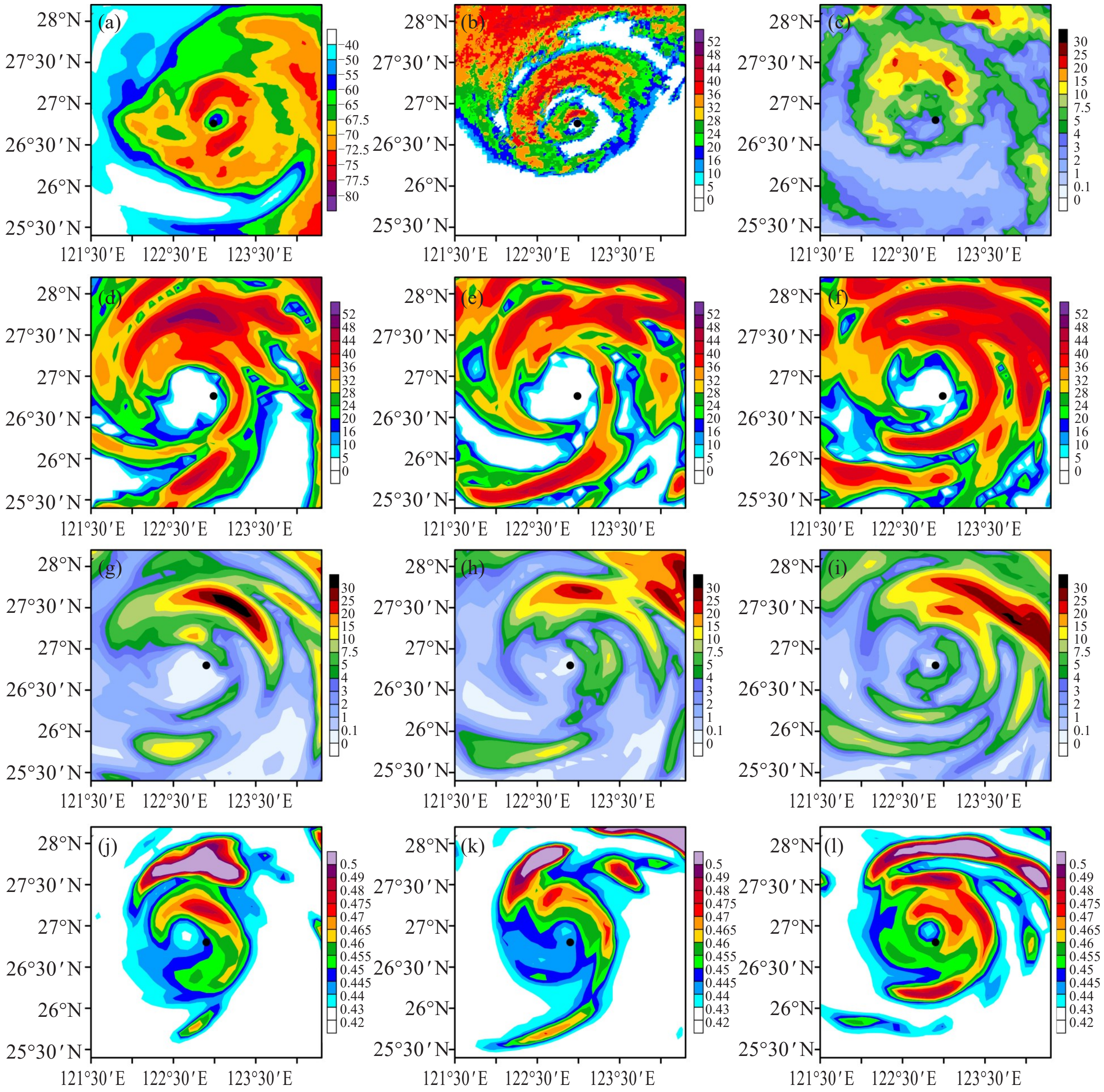

Figure 8. Same as Fig. 7 but showing the core area of Typhoon Lekima.

4.4 *Impacts on model initialization*

As shown in Figs. 4 and 6, the impact of vortex relocation and wind adjustment on typhoon simulation is large at the very beginning, but the effects of the absorbed observational information are dissipated over a short period, although Exp. IAU maintain this advantage for a longer time. This phenomenon is caused by inconsistencies between the ICs and model dynamics in Exp. VOR, which excite spurious high-frequency gravity wave noise during the first few hours of the model integration. As mentioned by both Polavarapu et al.[26] and Lee et al.[28], this spurious noise might cause initialization and spin-up problems, which are extremely harmful in the 3D variational method without model constraints. Clayton and Polavarapu et al. have presented rigorous mathematical proof that the filtering properties of the IAU technique are similar to those of the digital filter initialization technique (Lynch and Huang[39]), and thereby the IAU approach could resolve the problem of spurious noise[26, 40]. The tendencies of the model variables in all three experiments are shown in Fig. 9. A huge jump can be seen at the time of implementation of the vortex relocation and wind adjustment procedures in Exp. VOR. This big shock disappears in Exp. IAU because the increments are added gradually during the 3-h time window in each model step. This proves that use of the IAU technique in a typhoon initialization scheme is efficacious in resolving the problem of spurious high-frequency noise, which allows the model to reach equilibrium as soon as possible with minimal demand on computing resources.

5 CONCLUSIONS AND DISCUSSION

In this study, a typhoon initialization scheme based on the IAU technique was implemented in the ZJWARRS. Eight cycles of the ZJWARRS were conducted at 3-h intervals to investigate the impact of the typhoon initialization scheme on the simulated results for Typhoon Lekima (2019). The results of two numerical sensitivity experiments: Exp. VOR (which included implementation of vortex relocation and wind speed adjustment procedures) and Exp. IAU (which incorporated the IAU technique) were compared with the results of Exp. CTL (a simulation without any typhoon initialization scheme). The increments from the vortex relocation and wind speed adjustment procedures were absorbed at one time in Exp. VOR, whereas they were treated as constant forcing in the prognostic equations over the 3-h time window in Exp. IAU. The effects of the new typhoon initialization scheme on the initial fields and the prediction of typhoon track, intensity, and structure were investigated.

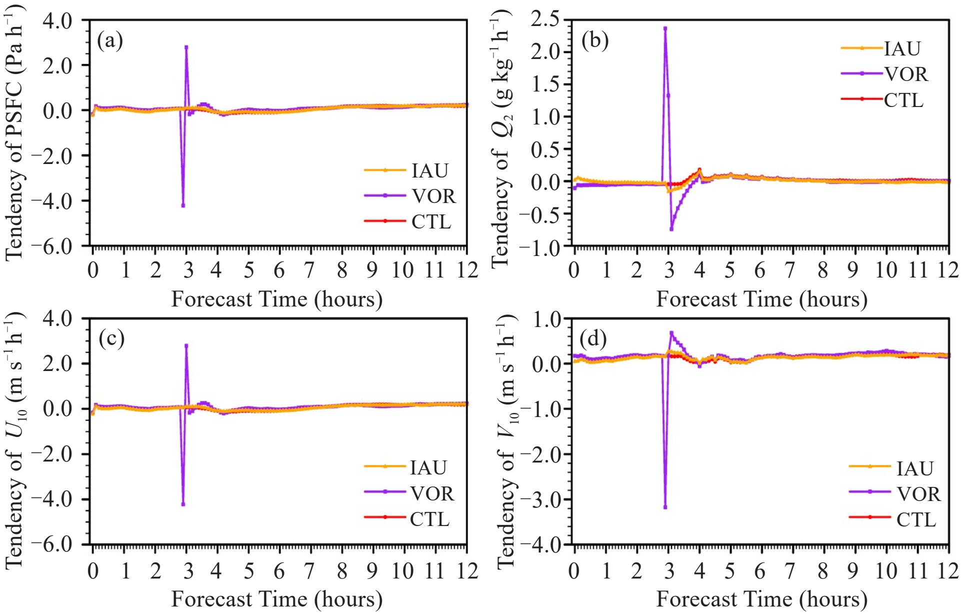

Figure 9. Comparison of simulated tendency of (a) surface pressure (Pa h^{-1}), (b) water vapor mixing ratio at 2 m (g kg^{-1} h^{-1}), (c) zonal wind speed at 10 m (m s^{-1} h^{-1}), and (d) meridional wind speed at 10 m (m s^{-1} h^{-1}).

Comparison of the initial fields in Exp. VOR with Exp. CTL revealed that the simulated typhoon position was corrected to the observed location by the vortex relocation procedure, and that the wind speed near the TC center was much larger following implementation of the wind adjustment procedure. Although the typhoon position and wind speed simulated in Exp. IAU were not as good as in Exp. VOR, Exp. IAU produced greater consistency in terms of other variables and the model dynamics. The vortex relocation and wind adjustment procedures improved the typhoon track and intensity in the first 6-h period in Exp. VOR, while these improvements were extended throughout the first 12-h period by the IAU technique in Exp. IAU.

The typhoon structure was also improved by the new typhoon initialization scheme, especially in Exp. IAU. The MWS was larger and the warm core of the typhoon was more obvious in Exp. IAU than in Exp. CTL in the first 12 h. All three experiments successfully reproduced the distribution of the spiral rain band, but the eye of the typhoon simulated in Exp. IAU was better organized. Further diagnosis of the tendencies of the variables revealed that the use of the IAU technique in the typhoon initialization scheme was efficacious in resolving the problem of spurious high-frequency noise, which allowed the model to reach equilibrium as soon as possible with minimal demand on computing resources.

In summary, a typhoon initialization scheme is important in typhoon numerical prediction, especially when the typhoon intensity of the background field is much weaker than observed. The typhoon initialization scheme based on the IAU technique used in this work not only adjusted the position and intensity of Typhoon Lekima (2019) closer to the observations, but also reduced the imbalance between the ICs and model dynamics. However, certain problems remain and will need further research. For example, the vortex relocation and wind speed adjustment procedures need further improvement to overcome the problem caused by the terrain-height condition, which might have substantial effect on the low-level wind distribution (Hsiao et al. [22]). The IAU time window adopted in this study was set to the same length as that in Xu et al. [32]; however, it could be sensitive to specific typhoon cases, which is a subject that will be explored further in future studies.

Acknowledgments: The authors would like to thank the European Centre for Medium-Range Weather Forecasts for the Integrated Forecasting System data, the Shanghai Typhoon Institute for the best-track data, and the China Meteorological Administration for the FY2G TBB, observed radar composite reflectivity, and CLDAS precipitation data. We thank James Buxton MSc from Liwen Bianji, Edanz Group China, for editing the English text of this manuscript.

REFERENCES

[1] LORENZ E N. A study of the predictability of a 28-variable atmospheric model [J]. Tellus, 1965, 17: 321-333, https://doi.org/10.1111/j.2153-3490.1965.tb01424.x.

[2] LORENZ E N. Deterministic nonperiodic flow [M]// HUNT B R, et al. (eds), The Theory of Chaotic Attractors, New York: Springer, 2004, 25-36.

[3] YAN Jing-hua, MAJEWSKI D. Experimental study of the role of initial and boundary conditions in mesoscale numerical weather prediction [J]. J Trop Meteor, 2003, 9 (2): 134-142.

[4] HUANG Yan-yan, CHEN Zi-tong, DAI Guang-feng, et al. Investigation on effects of initial schemes for binary typhoons Roke and Sonca in 2011 [J]. J Trop Meteor, 2016, 22(S1): 1-14, https://doi. org / 10.16555 / j. 1006-8775.2016.S1.001.

[5] WAN Qi-lin, XU Jian-jun, HE Jin-hai. Impacts of ATOVS data assimilation on prediction of a rainstorm over southeast China [J]. J Trop Meteor, 2009, 15(2): 155-161.

[6] HENDRICKS E A, PENG M S, LI T. Evaluation of multiple dynamic initialization schemes for tropical cyclone prediction [J]. Mon Wea Rev, 2013, 141(11): 4028-4048, https://doi.org/ https://doi.org/10.1175/MWR-D-12-00329.1.

[7] KURIHARA Y, BENDER M A, TULEYA R E, et al. Prediction experiments of Hurricane Gloria (1985) using a multiply nested movable mesh model [J]. Mon Wea Rev, 1990, 118(10): 2185-2198, https://doi.org/10.1175/1520-0493(1993)121<2030:AISOHM>2.0.CO;2.

[8] LORD S J. A bogussing system for vortex circulations in the National Meteorological Center Global Forecast Model [C]// 19th Conference on Hurricanes and Tropical Meteorology, Miami, FL, Amer Meteor Soc, 1991, 328-330.

[9] THU T, KRISHNAMURTI T. Vortex initialization for typhoon track prediction [J]. Meteorol Atmos Phys, 1992, 47(2): 117-126, https://doi.org/10.1007/BF01025612.

[10] WEN Xiao-pei, LONG Xiao, ZHANG Shu-wen, et al. Numerical studies of planetary boundary layer parameterization schemes on Super Typhoon Sanba(2012) during its initial stage [J]. J Trop Meteor, 2018, 24(3): 288-299, https://doi. org / 10.16555 / j. 1006-8775.2018.03.003.

[11] KURIHARA Y, BENDER M A, ROSS R J. An initialization scheme of Hurricane Models by vortex specification [J]. Mon Wea Rev, 1993, 121(7): 2030-2045, https://doi.org/10.1175/1520-0493(1993)121<2030:AISOHM>2.0.CO;2.

[12] KURIHARA Y, BENDER M A, TULEYA R E, et al. Improvements in the GFDL hurricane prediction system [J]. Mon Wea Rev, 1995, 123(9): 2791-2801, https://doi.org/10.1175/1520-0493(1990)118<2185:peohgu>2.0.co;2.

[13] BENDER M A, GINIS I, TULEYA R, et al. The operational GFDL coupled Hurricane-Ocean Prediction System and a summary of its performance [J]. Mon Wea Rev, 2007, 135(12): 3965-3989, https://doi.org/10.1175/2007MWR2032.1.

[14] LIU Q F, MARCHOK T, PAN H L, et al. Improvements in Hurricane Initialization and Forecasting at NCEP with Global and Regional (GFDL) Models [DB/OL]//NCEP/EMC TECH Procedures Bull. 472, 2000, 7 pp. [Available online at http://205.156.54.206/om/tpb/472.htm].

[15] YUAN J, SONG L L, HUANG Y Y, et al. A method of initial vortex relocation and numerical simulation experiments on tropical cyclone track [J]. J Trop Meteor, 2011, 17(1): 36-42, https://doi.org/10.3969/j.issn.1006-8775.2011.01.005.

[16] XIAO Q, ZOU X, WANG B. Initialization and simulation of a landfalling hurricane using a variational bogus data assimilation scheme [J]. Mon Wea Rev, 2000, 128(7): 2252-2269, https://doi.org/10.1175/1520-0493(2000)128<2252:IASOAL>2.0.CO;2.

[17] PU Z X, BRAUN S A. Evaluation of bogus vortex techniques with four-dimensional variational data assimilation [J]. Mon Wea Rev, 2001, 129(8): 2023-2039, https://doi. org / 10.1175 / 1520-0493(2001)129<2023:eobvtw>2.0.co;2.

[18] HUANG Yan-yan, YAN Jing-hua, MENG Wei-guang, et al. Improvement of summer high temperature forecasting in Guangzhou during the typhoon period using a BDA scheme [J]. Acta Meteor Sin, 2010, 68(1): 102-113(in Chinese), https://doi.org/10.11676/qxxb2010.011.

[19] YUAN Bing, FEI Jian-fang, WANG Yun-feng, et al. Experimental study on a dynamic asymmetrical typhoon initialization scheme based on 4D-Var [J]. J Trop Meteor, 2010, 16(4): 363-371, https://doi.org/10.3969/j.issn.1006-8775.2010.04.008.

[20] QU An-xiang, MA Su-hong, LIU Qing-fu, et al. The initialization of tropical cyclones in the NMC global model, Part II: Implementation [J]. Acta Meteor Sin, 2009b, 67(5): 727-735(in Chinese), https://doi. org / 10.11676/qxxb2009.073.

[21] QU An-xiang, MA Su-hong, LIU Qing-fu, et al. The initialization of tropical cyclones in the NMC global model, Part I: Scheme design [J]. Acta Meteor Sin, 2009a, 67(5): 716-726(in Chinese), https://doi. org / 10.11676 / qxxb2009.072.

[22] HSIAO L F, LIOU C S, YEH T C, et al. A vortex relocation scheme for tropical cyclone initialization in advanced research WRF [J]. Mon Wea Rev, 2010, 138(8): 3298-3315, https://doi.org/10.1175/2010mwr3275.1.

[23] LIANG Xu-dong, WANG Bin. Data assimilation cycle experiments in typhoon numerical prediction using the model constrained 3DVar [J]. Acta Meteor Sin, 2010, 68 (2): 153-161(in Chinese), https://doi. org / 10.11676 / qxxb2010.016.

[24] HUANG Wei, LIANG Xu-dong. A cycling typhoon like vortex initialization scheme and its application to GRAPES-TCM [J]. Acta Meteor Sin, 2010, 68(3): 365-375(in Chinese), https://doi.org/10.11676/qxxb2010.036.

[25] BLOOM S C, TAKACS L L, SILVA A M, et al. Data

assimilation using incremental analysis updates [J]. Mon Wea Rev, 1996, 124(6): 1256-1271, https://doi. org/10.1175/1520-0493(1996)124<1256:dauiau>2.0.co;2.

[26] POLAVARAPU S, REN S, CLAYTON A M, et al. On the relationship between incremental analysis updating and incremental digital filtering [J]. Mon Wea Rev, 2004, 132 (10): 2495-2502, https://doi.org/10.1175/1520-0493(2004)132<2495:otrbia>2.0.co;2.

[27] TAKACS L L, SUÁREZ M J, TODLING R. The stability of incremental analysis update [J]. Mon Wea Rev, 2018, 146(10): 3259-3275, https://doi.org/10.1175/MWR-D-18-0117.1.

[28] LEE M S, KUO Y H, BARKER D M, et al. Incremental analysis updates initialization technique applied to 10-km MM5 and MM5 3DVAR [J]. Mon Wea Rev, 2006, 134 (5): 1389-1404, https://doi.org/10.1175/mwr3129.1.

[29] OURMIÈRES Y, BRANKART J M, BERLINE L, et al. Incremental analysis update implementation into a sequential ocean data assimilation system [J]. J Atmos Ocean Tech, 2006, 23(12): 1729-1744, https://doi. org /10.1175/jtech1947.1.

[30] BENKIRAN M, GREINER E. Impact of the incremental analysis updates on a real-time system of the North Atlantic Ocean [J]. J Atmos Ocean Tech, 2008, 25(11): 2055-2073, https://doi.org/10.1175/2008JTECHO537.1.

[31] LEI L, WHITAKER J S. A four-dimensional incremental analysis update for the ensemble kalman filter [J]. Mon Wea Rev, 2016, 144(7): 2605-2621, https://doi. org /10.1175/mwr-d-15-0246.1.

[32] XU Dao-sheng, ZHANG Bang-lin, ZENG Qing-cun, et al. A typhoon initialization scheme based on incremental analysis updates technology [J]. Acta Meteor Sin, 2019, 77(6): 1053-1061 (in Chinese), https://doi.org/10.11676/qxxb2019.060.

[33] SKAMAROCK W C, KLEMP J B, DUDHIA J, et al. A Description of the Advanced Research WRF Model Version 4 [DB / OL]//NCAR TECHNICAL NOTE / TN-556 + STR, 2019, 145 pp. [Available online at https://www2. mmm. ucar. edu / wrf / users / docs / technote / v4_technote.pdf].

[34] CHEN Feng, DONG Mei-ying, JI Chun-xiao, et al. Evaluation of the summer precipitation and temperature forecast by WRF model in Zhejiang in 2011 and its sensicitivity to wet processes [J]. J Zhejiang Meteor, 2012, 33(3): 3-12(in Chinese), https://doi.org/10.3969/j.issn.1004-5953.2012.03.002.

[35] QIU Jin-jing, CHEN Feng, DONG Mei-ying, et al. Establishment and evaluation of Zhejiang WRF-ADAS Rapid Refresh System [J]. Adv Meteor Sci Technol, 2015, 5(6): 6-12(in Chinese), https://doi. org / 10.3969 / j.issn.2095-1973.2015.06.001.

[36] XUE M, DROEGEMEIER K K, WONG V. The Advanced Regional Prediction System (ARPS) – A multi-scale nonhydrostatic atmospheric simulation and prediction model, Part I: Model dynamics and verification [J]. Meteor Atmos Phys, 2000, 75(3): 161-193, https://doi.org/10.1007/s007030070003.

[37] XUE M, DROEGEMEIER K K, WONG V, et al. The Advanced Regional Prediction System (ARPS) – A multi-scale nonhydrostatic atmospheric simulation and prediction tool, Part II: Model physics and applications [J]. Meteor Atmos Phys, 2001, 76(3): 143-165, https://doi.org/10.1007/s007030170027.

[38] BREWSTER K. Application of a bratseth analysis scheme including doppler radar data [C]// 15th Conference on Weather Analysis and Forecasting, Norfolk, VA, USA, 1996: 92-95.

[39] LYNCH P, HUANG X Y. Initialization of the HIRLAM model using a digital filter [J]. Mon Wea Rev, 1992, 120 (3): 1019-1034, https://doi.org/10.1175/1520-0493(1992)1202.0.CO;2.

[40] CLAYTON A. Incremental Analysis Update (IAU) Scheme [R]. Unified Model Documentation Paper 31, UK Met Office, 2003, 20pp.

Citation: CHEN Feng, DONG Mei-ying, JI Chun-xiao, et al. Application of a typhoon initialization scheme based on the incremental analysis updates technique in a rapid update cycle system [J]. J Trop Meteor, 2020, 26(4): 428-440, https://doi.org/10.46267/j.1006-8775.2020.037.